Research Square

Preprints are preliminary reports that have not undergone peer review.
They should not be considered conclusive, used to inform clinical practice,
or referenced by the media as validated information.

Beyond the Group Average: Interindividual Variability in Neural Activity During Written Word Processing

Eva Philomena Steckermeier

eva.steckermeier@plus.ac.at

University of Salzburg

Mario Braun

University of Salzburg

Florian Hutzler

University of Salzburg

Martin Kronbichler

University of Salzburg

Research Article

Keywords: Witten word processing, language processing, precision fMRI, individual variability, multi-echo fMRI

Posted Date: November 19th, 2026

DOI: https://doi.org/10.21203/rs.3.rs-11350881/v1

License: This work is licensed under a Creative Commons Attribution 4.0 International License.
Read Full License

Additional Declarations: No competing interests reported.

Beyond the Group Average: Interindividual Variability in Neural Activity During Written Word Processing

Eva Philomena Steckermeier[1,2] (https://orcid.org/0009-0004-8516-7738)

Mario Braun[1,2] (https://orcid.org/0000-0001-5054-4960)

Florian Hutzler[1,2] (https://orcid.org/0000-0001-8195-4911)

Martin Kronbichler[1,2,3] (https://orcid.org/0000-0003-2240-2812)

[1]Centre for Cognitive Neuroscience, University of Salzburg, Salzburg, Austria

[2]Department of Psychology, University of Salzburg, Salzburg, Austria

[3]Neuroscience Institute, Christian-Doppler University Hospital, Paracelsus Medical University, Salzburg, Austria

Corresponding author:
Eva P. Steckermeier, eva.steckermeier@plus.ac.at

Acknowledgements:

The authors gratefully acknowledge the data storage infrastructure and organisational support provided by the ANC, as well as the computational resources and services offered by Salzburg Collaborative Computing (SCC), funded by the BMBWF and the State of Salzburg. This research also benefited from the use of the PsychoPy-BIDS plugin, which facilitated the integration of our experimental design with BIDS-compatible data formats.

Abstract

The processing of language and reading has been a subject of interest for neuropsychologists for many decades. Nevertheless, variability between subjects within the language network has received comparatively little attention. In this study, we employed a precision fMRI approach to examine between-subject variability in neural activity during single-word reading. In order to assess the similarity between subjects' activation patterns, two methods were utilised: Spearman's rank correlation and the Jaccard index. Following this, an exploratory correlation was performed between the similarity and subjects' characteristics. As part of the quantification of between-subject variance, the brain regions characterised by the most variance were identified using interclass correlation coefficients (ICC). The participants exhibited a moderate similarity in their activation patterns, which was correlated with their reading performance and psychopathological traits. Brain regions exhibiting notably high interindividual variability were predominantly located within or adjacent to the language network, suggesting variability in the precise location and extent of the language network among subjects. A comparison of the group-level activation map derived from the same sample revealed that it provided only a moderate representation of the individual maps. The findings underscore the significance of integrating group-level analyses with individual-centred methodologies to achieve more precise characterisation of the neural organisation of language and advance our understanding of the brain-behaviour relation.

Keywords: Witten word processing, language processing, precision fMRI, individual variability, multi-echo fMRI

f

1. Introduction

While you are reading these words, your brain is rapidly transforming visual symbols into meaningful language. Within a fraction of a second, letters and words are identified and linked to stored linguistic knowledge, forming coherent representations of meaning. Although this process appears effortless, it requires the coordinated activity of multiple cortical regions to transform visual input into these complex linguistic representations. This process involves a predominantly left-lateralised cortical network supporting orthographic processing, phonological decoding, lexical retrieval, and semantic integration.

Key regions of the language network include the inferior frontal gyrus (IFG), the middle frontal gyrus (MFG), the superior frontal gyrus (SFG), the supplementary motor area (SMA), precentral gyrus superior temporal gyrus (STG), the angular gyrus (AnG), the middle temporal gyrus (MTG), the ventral occipitotemporal cortex (vOT) including the visual word form area (VWFA), the supramarginal gyrus (SMG), and the early visual cortex including the calcarine cortex, the lingual gyrus, and the cuneus (Braga et al. 2020; Fedorenko et al. 2024; Glezer et al. 2016; Hodgson et al. 2021; Liu et al. 2024; Liuzzi et al. 2019; Yu et al. 2018; Yuan et al. 2023; Ludersdorfer et al. 2016; Moliadze et al. 2021; Pattamadilok et al. 2017; Planton et al. 2019; Turker et al. 2023; Weber et al. 2020). Additionally, also parts of the right cerebellum are believed to play a role in various language-related processes (Martin et al. 2015; Casto et al. 2026).

Research into the language network mostly relies upon group-study designs. Although such approaches are useful for identifying where language is processed in the brain and for generating a model of the average neurotypical brain, they do not provide information on how this activation translates into actual interindividual neural activity or individual reading performance. This is critical for the following reasons: First, emphasising sampling many individuals often limits the data available from each participant, thereby reducing the amount of information that can be used to reliably characterise individual activation patterns. Second, a significant group-level effect may be driven primarily by a subset of participants exhibiting particularly strong responses without indicating how consistently the activity is expressed across individuals (Elliott et al. 2021; Korucuoglu et al. 2020; Lynch et al. 2021; Poldrack 2017). Third, interindividual variability is often dismissed as noise rather than being recognised as a potentially meaningful feature of neural organisation (Michon et al. 2022; Seghier and Price 2018). However, it is essential to characterise the nature and extent of interindividual variability in order to accurately interpret group-level findings. The next step in cognitive neuroscience is therefore to move from attempting to identify general models of cognitive processes to applying these models to individual subjects.

Previous research demonstrated that variations in brain activation might shed light on brain-behaviour associations in reading: For instance, variations in neural responses during language and reading tasks have been linked to differences in reading ability, inhibitory control, and general cognitive ability (Braga et al. 2020; Weber et al. 2020; Liu et al. 2024; Prat et al. 2023; Yamasaki and Prat 2023; Cui et al. 2018; Granocchio et al. 2021; Jung et al. 2019; Spencer and Cutting 2021; Xu et al. 2020; Zhang et al. 2020). Further evidence suggests that variation in language-related neural responses may also be associated with psychopathological factors: For example, higher levels of positive schizotypy have been linked to reduced cerebellar activity during visual word recognition. Similarly, individual differences in facets of psychopathy, such as boldness, meanness and motor impulsivity, have been linked to variations in neural activity during lexical decision-making (Vanova et al. 2020).

To accurately map how these diverse cognitive and psychopathological traits manifest in the brain, it is necessary to resolve functional networks at the single-subject level. Precision fMRI achieves this by moving away from group templates and provides a fuller picture of neural activity by recognising and understanding both commonalities and differences between individuals (Fedorenko 2021; Gratton et al. 2020; Smith et al. 2021; Laumann et al. 2015). Precision fMRI and the description of the individual organization of brain network requires a different sampling strategy, emphasizing data quality and quantity on the individual subject level. To date, several proof-of-concept studies show that precision fMRI is able to move us towards an individualized understanding of brain activation: With four participants Fedorenko et al. (2024) illustrated considerable variation between individuals in the location, shape, and extent of language-related activation. However, the sample size of four individuals was remarkedly small. Meanwhile, Braga et al. (2020) demonstrated the value of precision mapping in functional connectivity analysis by characterising the organisation of language-related networks within individuals and by distinguishing spatially adjacent association networks that are difficult to separate at the group level. While these pioneering studies highlight the potential of precision fMRI, their limitations include small sample sizes and a failure to investigate individual functional activation patterns and their similarity between subjects. Furthermore, they do not examine the extent to which group-level patterns reflect underlying individual activations.

The present study aims to fill this gap by adopting a precision fMRI approach across four sessions to assess the neural activity during word reading. To maximize data quality at the single-subject level without extending scan time, multi-echo fMRI is used to significantly improve the signal-to-noise ratio and reduce motion artefacts (Elliott et al. 2021; Kirilina et al. 2016; Kundu et al. 2017; Steel et al. 2022). It also allows for additional denoising using advanced preprocessing tools such as tedana (DuPre et al. 2021), which uses multi-echo

Independent Component Analysis (ME-ICA) to distinguish noise from the blood-oxygen-level-dependent (BOLD) response (Caballero-Gaudes et al. 2019; DuPre et al. 2021; Moia et al. 2021; Steel et al. 2022; Lynch et al. 2020; Kundu et al. 2017). Crucially for language research, this approach mitigates signal dropouts in key inferior frontal regions (Kundu et al. 2017; Caballero-Gaudes et al. 2019; Elliott et al. 2021; Kirilina et al. 2016; Steel et al. 2022). Due to their location, their relaxation times differ from those of more dorsal regions. These inaccuracies in capturing the signal in its entirety for these regions may have led to inconsistent findings regarding the involvement of these areas in different processes.

Taken together, our approach is the first that allows to: 1. examine aspects of the similarity between participants in relative activity patterns and their spatial distribution. 2. identified regions demonstrating the greatest variance between subjects (allowing us to determine which regions exhibit relatively stable versus more variable functional organisation). 3. explored the relationship between similarity in functional activity between individuals and their characteristics, including task performance, reading ability, general cognitive ability, and mental health. 4. examine variability between subjects regarding the lateralisation of functional activity, since it has been found that approximately 7–10% of the population exhibit atypical right- or bi-lateralisation of the language network (Seghier and Price 2018; Andrulyte et al. 2026). 5. compare individual activity patterns with group-level results derived from the same data, to determine the extent to which group-level patterns reflect the functional organisation of individual subjects.

This study builds on previous precision fMRI studies to strengthen the empirical basis for evaluating the relevance of interindividual variability when interpreting findings and models derived from group-level study designs. Furthermore. It indicates factors that may contribute to interindividual differences in neural activity during reading, even among a seemingly homogeneous population of healthy students.

2. Methods

We used the dataset the ANC language study (Steckermeier et al. 2025a; Steckermeier et al. 2026), which can be found on the Austrian NeuroClound (Austrian NeuroCloud, 2026, September) (https://doi.org/10.60817/39tp-6031). The following section will focus on parts relevant for this work.

2.1 Participants

We included 21 subjects of the dataset with exclusions due to incomplete data or technical issues while preprocessing (sub-s016 and sub-s018). They were 19 – 31 years old (M = 24.62, SD = 3.14, 14 female and 7 male). All were right-handed native German speakers with no neurological or psychiatric disorders reported, and a secondary

education (A-levels) or higher. The study was approved by the local ethics committee of the University of Salzburg and conducted in accordance with the Declaration of Helsinki. All subjects gave an informed consent to participating in the study as well as data sharing and reuse.

2.2 Cognitive Measures and Psychopathological Screening

Reading performance was assessed using the Salzburger Lesescreening (SLS) (Lüdtke et al. 2019) and the oral reading task of the Salzburger Lese- und Rechtschreibtest II (SLRT II) (Salzburger Reading- and Orthographytest) (Moll and Landerl 2014). General cognitive ability was estimated using the Vocabulary, Matrix Reasoning, Coding, and Digit Span subtests of the German version of the Wechsler Adult Intelligence Scale (WAIS-IV) (Petermann 2018). We screened for psychopathology using the self-assessment Adult Self Report (ASR) (Achenbach and Rescorla 2003).

2.3 Task

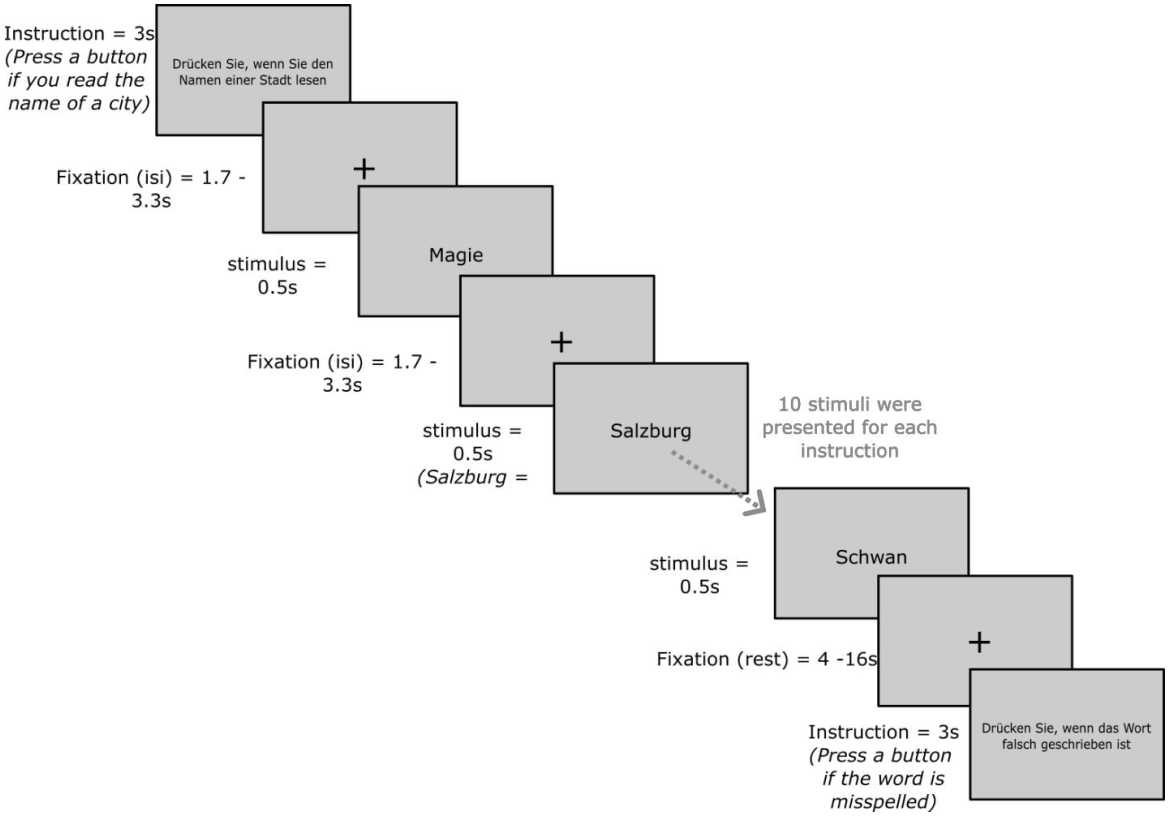
We used the ANC-Language study's visual word discrimination task. This task comprises four subtasks: semantic, phonological and orthographic discrimination as well as a control condition. The word category and rhyme judgement tasks engage brain regions associated with semantic and phonological processing respectively (Billingsley et al. 2001; Seghier et al. 2004; Wagley and Booth 2022). Orthographic processing was assessed using a misspelling detection task (Kronbichler et al. 2007). In the control condition, letter clusters were presented in a false font (Hawelka and Wimmer 2008). Thus, although the stimuli visually resembled words, they were unintelligible because they consisted of unfamiliar characters, thereby controlling for visual input and general task demands.

Each run of the word discrimination task lasted approximately 14.5 minutes and comprised 20 blocks. Each block began with a 3-s instruction cue indicating the upcoming subtask, followed by the presentation of 10 single words (0.5 s each). The stimuli were separated by fixation crosses with a jittered duration ranging from 1.7 to 3.3 s (mean = 2.5 s). Each block contained one or two target stimuli and ended with an extended fixation period lasting 4 to 16 s (mean = 8 s). Participants were instructed to respond to target stimuli as quickly and accurately as possible by pressing a button. The analyses only included non-target stimuli for which no response was correctly given.

The word discrimination task was implemented in Python using PsychoPy (v2023.1.0) together with the psychopy-bids plugin (v2023.1.1). The task was displayed on a 32-inch BOLDscreen LCD monitor (Cambridge Research Systems; 1920 × 1080 pixels, 120 Hz) and viewed through a mirror attached to the MRI head coil. The viewing distance was approximately 190 cm.

Fig. 1

The visual word discrimination task



2.4 Stimuli

All word discrimination tasks used German nouns. A total of 1,020 non-target words were divided into three sets of 340 words each. The sets were matched for a range of lexical, psycholinguistic, and affective properties to ensure comparable stimulus characteristics. For a detailed description of the procedure, matching criteria, and complete lists, please refer to the ANC Language study publications (Steckermeier et al. 2025b; Steckermeier et al. 2026). The assignment of the three stimulus sets to the tasks was randomised across participants. In addition, 240 target words were included to elicit button-press responses.

2.5 MRI Acquisition

The study comprised four scanning sessions, each lasting approximately 1.5 hours. The MRI data were acquired using a 3 Tesla Siemens Prisma-fit MRI (Siemens AG, Erlangen, Germany) located at the Christian Doppler University Hospital in Salzburg, Austria. A 20-channel head coil was used. Functional MRI data sensitive to BOLD contrast were collected during the two runs of the visual word discrimination task using T2*-weighted gradient multi-echo axial EPI sequences with four echoes (TR=1299ms, TE1=12.40ms,

TE2=30.13ms, TE3=47.86ms, TE4=65.59ms, matrix=78×78, FOV=192mm, flip angle=77°, number of slices=56, voxel size=2.5×2.5×2.5mm, MB factor=4, iPAT factor=2 (GRAPPA)). Further sequences relevant for this work are the gradient echo field map (TR=623ms, TE1=4.92ms, TE2=7.38ms, voxel size=2.5×2.5×2.5mm) and the high-resolution anatomical T1-weighted MP-RAGE scan (TR=2400ms, TE=2.24ms, flip angle=8°, TI=1060ms, voxel size=0.8×0.8×0.8mm, iPAT factor=2 (GRAPPA)) acquired in each session.

2.6 MRI Data preprocessing

MRI data were pre-processed using fMRIPrep (v24.1.1) (Esteban et al. 2019). The pipeline was run using the longitudinal workflow, with T1-weighted images serving as reference for BOLD-to-anatomical registration. Functional data were normalised to MNI152NLin6Asym standard space at 2 mm isotropic resolution. The single echo images were retained and processed using tedana (v25.0.1) (DuPre et al. 2021) for multi-echo denoising using the default tedana workflow. After coregistration and normalization using advanced normalization tools (ANTs), the resulting denoised and combined functional images were prepared for statistical analysis by smoothing using SPM12 with a Gaussian kernel of 6 × 6 × 6 mm full width at half maximum (FWHM).

2.7 MRI Data Analysis

2.7.1 First-level analysis

SPM12 (MATLAB R2013a) was used to perform first-level single-subject analyses using a fixed-effects model. The statistical models were estimated separately at two levels, resulting in activation maps at both the session and subject levels.

2.7.2 Between subject similarity

We used the PyReliMRI (2.2.2) toolbox in a Python (3.13.5) environment to assess whole-brain variability. We calculated the similarity using two statistical approaches: (1) Spearman's rho, reflecting voxelwise activation patterns, and (2) the Jaccard coefficient, reflecting spatial overlap. For the Spearman's rho, we correlated unthresholded contrast images from the first-level analysis, and for the Jaccard correlation, we used the respective thresholded ($p < .001$, $k = 0$) contrast images.

Several factors were explored on an exploratory basis to determine whether they contribute to interindividual variability in neural activity. We assessed if the similarity coefficients were related to noise parameters using MRIQC (Esteban et al. 2017) measurements from the ANC-language study dataset (Steckermeier et al. 2025b). We selected framewise displacement, signal-to-noise ratio (SNR), temporal signal-to-noise ratio (tSNR), DVARS, entropy-focus criterion (EFC), foreground-to-background energy ratio

(FBER), and full-width at half maximum (FWHM) as noise indicators. We extracted the parameters for the visual word discrimination task and correlated these subject means with the subject similarity coefficients. Next, we examined potential relations between similarity coefficients and subject characteristics: task performance, response speed, age, education, reading ability, general intelligence, and psychopathological screening scores.

2.7.3 Most Between Subject Variance

To identify brain regions showing reliable between-subject differences, we combined voxelwise estimates of between-subject variance with their reliability across sessions. Specifically, the voxelwise intraclass correlation coefficient (ICC(3,1)) was calculated using PyReliMRI from the first-level contrast images across sessions and participants:

$$ICC(3,1)=Var_{between}/(Var_{between}-Var_{error})$$

where $Var_{between}$ represents the between-subject variance and Var_{error} the within-subject error variance. A brain mask comprising voxels present in all input images was generated using Nilearn (v0.12.0) and NiBabel (v5.3.2) and applied to the ICC calculation. To identify regions with both sufficient reliability and high between-subject variability, we applied an ICC threshold of >0.6. Separately, the 5% of voxels with the highest between-subject variance were identified. The final mask comprised the spatial overlap between these two criteria, yielding regions with both sufficient reliability and most between-subject variability.

We repeated the analysis workflow for the between subject similarity analysis for the most between subject variance mask, again calculating both, the Spearman and Jaccard similarity. Subsequently, we again correlated the similarity coefficients with the noise parameters, participants' characteristics, and psychopathological screening scores.

2.7.4 Lateralisation Index

Lateralisation of activity during visual word reading was assessed using the Laterality Index toolbox for SPM (Wilke and Lidzba 2007). The bootstrap thresholding method was used for LI estimation, with all lobes included in the inclusive mask. A midline exclusion mask of ±5 mm was applied to exclude activation close to the interhemispheric midline. Positive LI values indicate greater left- than right-hemispheric activation, whereas negative values indicate the opposite.

2.7.5 Group Level Analysis

The second-level group analysis was also performed with SPM12 using a random effects model. We then calculated the similarity between the group-level activation map and the

single-subject activation maps using PyReliMRI again. For the Spearman's rho, the unthresholded contrast images per subject obtained from the first-level analysis were correlated with the unthresholded contrast image from the group analysis. For the Jaccard correlation, the respective thresholded ($p < .001$, $k = 0$) contrast images were used.

3. Results

3.1 Between Subject Similarity

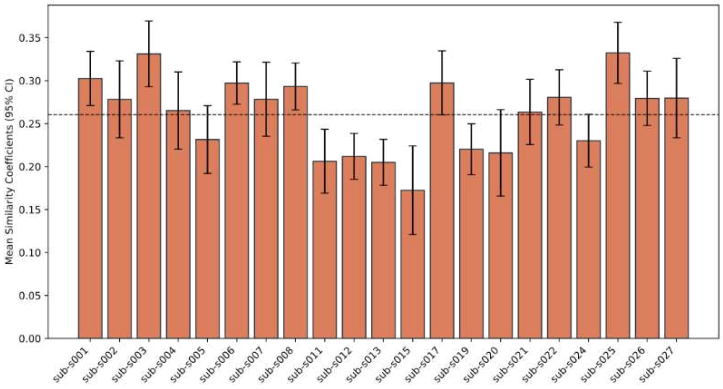
To assess the similarity of activation maps, two complementary measures were used: Spearman's rho (reflecting similarity in relative activation patterns) and the Jaccard coefficient (reflecting spatial overlap).

The mean rho was 0.26 (SD = 0.04), with a range width of 0.16. Subject sub-s015 showed the lowest mean similarity (rho = 0.172, SD = 0.11). Additional subjects with below-average similarity (more than one standard deviation below the group mean) were sub-s013 (rho = 0.205, SD = 0.06), sub-s011 (rho = 0.206, SD = 0.08), sub-s012 (rho = 0.212, SD = 0.06), and sub-s020 (rho = 0.216, SD = 0.11). The highest mean similarity was observed for subject sub-s025 (rho = 0.332, SD = 0.08), closely followed by subject sub-s003 (rho = 0.331, SD = 0.08). Compare Fig. 2.

Fig. 2

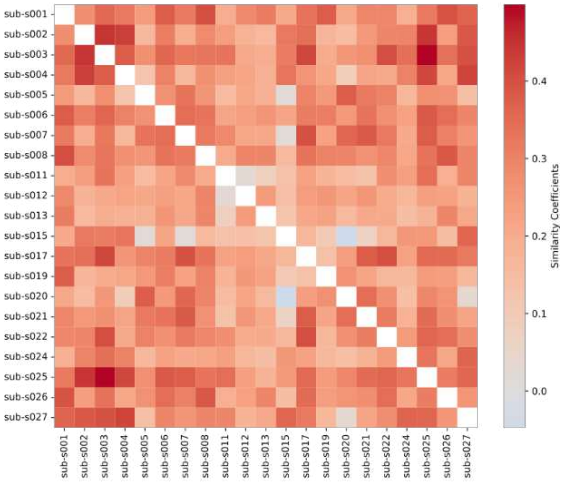
Spearman's rank (rho) Similarity Coefficients

a) Per Subject Mean Similarity Coefficient



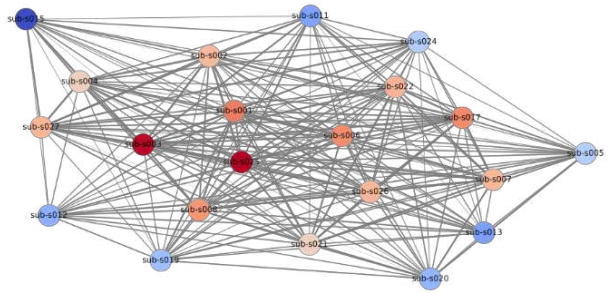
Mean Spearman's rank (rho) similarity coefficient for each subject over all pairwise comparisons including confidence intervalls (95%). Mean similarity was rho = 0.26 (SD=0.04), range=0.16. Smallest similarity showed subject sub-s015 with rho = 0.172, highest subject sub-s025 with rho = 0.332.

b) Subject x Subject Similarity Matrix



The matrix shows the Spearman Similarity Coeficients of the pairwise comparisons between subjects. Darker fields indicate a higher similarity, while lighter field present a lower similarity. The highest similarity was observed between subject sub-s003 and sub-s025 with rho = 0.499, the lowest similarity showed the comparison between subject sub-s015 and subject sub-s020 with rho = -0.047.

c) Network Representation of the Similarity Coefficients



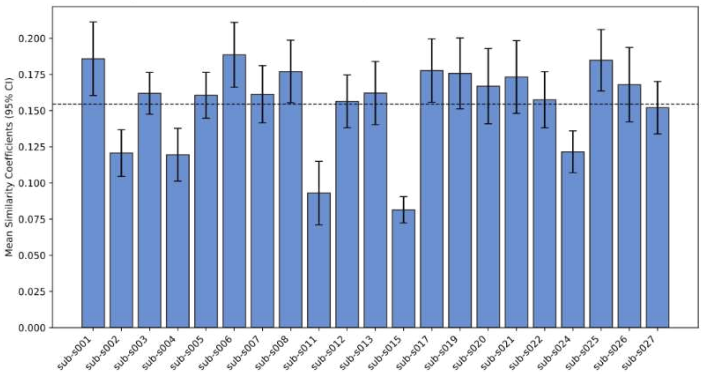
In this network the length and thickness of the connections between two subjects represent their similarity value, thus, thicker and shorter lines indicate higher similarity beetween two subjects, while thiner and longer lines illustate lower similarity.

Across all pairwise comparisons, the mean Jaccard coefficient (J) was J = 0.16 (SD = 0.03), with a range width of 0.11. Subject-specific mean pairwise similarity was lowest for subject sub-s015 (J = 0.082, SD = 0.02), followed by sub-s011 (J = 0.093, SD = 0.05), sub-s004 (J = 0.120, SD = 0.04), sub-s002 (J = 0.121, SD = 0.03), and sub-s024 (J = 0.122, SD = 0.03). The highest mean pairwise similarity was observed for sub-s006 (J = 0.189, SD = 0.05), followed by sub-s001 (J = 0.186, SD = 0.05) and sub-s025 (J = 0.185, SD = 0.05). Compare Fig. 3.

Fig. 3

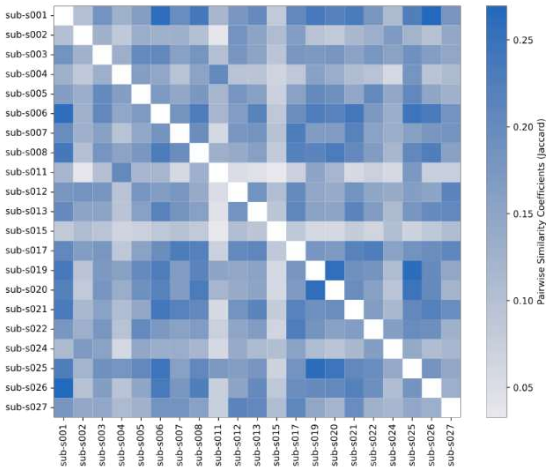
Jaccard Similarity Coefficients

a) Per Subject Mean Similarity Coefficient



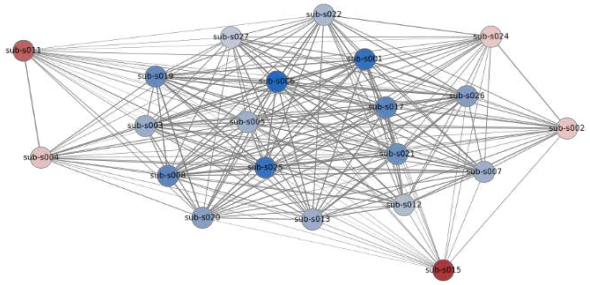
Mean Jaccard similarity coefficient for each subject over all pairwise comparisons including confidence intervalls (95%). Mean similarity was J = 0.16 (SD=0.03), range=0.11. Smallest similarity showed subject sub-s015 with J = 0.082, highest subject sub-s006 with J = 0.189.

b) Subject x Subject Similarity Matrix



The matrix shows the Jaccard Similarity Coeficients of the pairwise comparisons between subjects. Darker fields indicate a higher similarity, while lighter field present a lower similarity. The highest similarity was observed between subject sub-s001 and sub-s026 with J = 0.270, the lowest similarity showed the comparison between subject sub-s011 and sub-s015 with J = 0.033.

c) Network Representation of the Similarity Coefficient



In this network the length and thickness of the connections between two subjects represent their similarity value, thus, thicker and shorter lines indicate higher similarity beetween two subjects, while thiner and longer lines illustate lower similarity.

Neither similarity measure was significantly correlated with any of the assessed MRI quality metrics, including framewise displacement, SNR, tSNR, DVARS, EFC, FBER, and FWHM.

To see the individual-subject activation maps, refer to Fig. A1 and for the similarity values per subject, refer to Table A1 in Appendix.

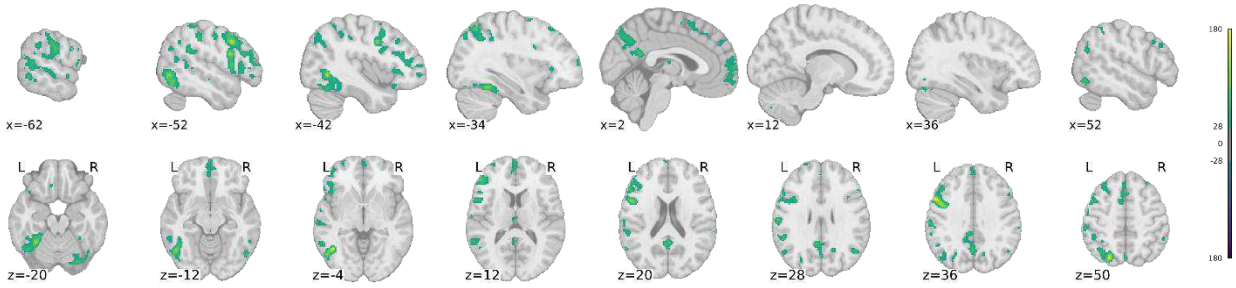
3.2 Most Between-Subject Variance

To identify the brain regions showing for most between-subject variance, a mask was created using ICC > 0.6 as cut off for quality control and extracting the voxels with the top 5% of between-subject variance. This mask included on the left hemisphere parts of the precentral gyrus, the IFG pars triangularis and opercularis, the fusiform gyrus, the MTG and

the STG, the superior parietal lobe (SPL), the postcentral gyrus, the SMG, the middle occipital gyrus (mOT), the MFG, the SMA, the AnG, and the plenum temporale. Regions included bilaterally were the inferior occipital gyrus (iOT), the cerebellum, and the ITG, compare Fig. 4.

Fig. 4

Regions showing the most between-subject variance



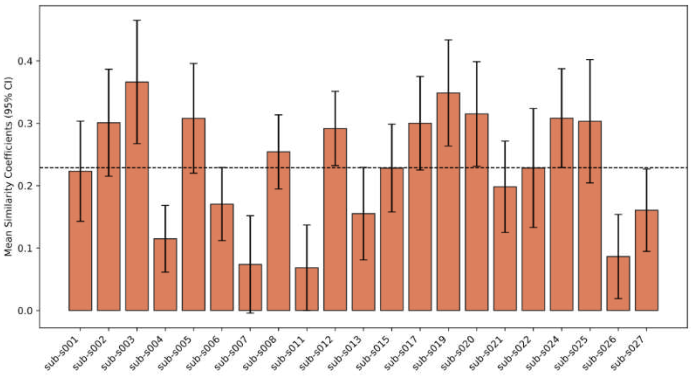
Regions showing the most between-subject variance reliably, identified with a mask including voxel with ICC>0.6 and top 5% between-subject variance.

We also investigated the similarity between subjects for these regions. The mean rho for the mask was 0.23 (SD = 0.09), with a range width of 0.30. Subject sub-s011 showed the lowest mean pairwise similarity (rho = 0.068, SD = 0.15). Other subjects with below-average similarity were sub-s007 (rho = 0.074, SD = 0.17), sub-s026 (rho = 0.086, SD = 0.14) and sub-s004 (rho = 0.115, SD = 0.11). The highest mean similarity was observed for subject sub-s019 (rho = 0.349, SD = 0.18), followed by subject sub-s003 (rho = 0.336, SD = 0.21), see Fig. 5.

Fig. 5

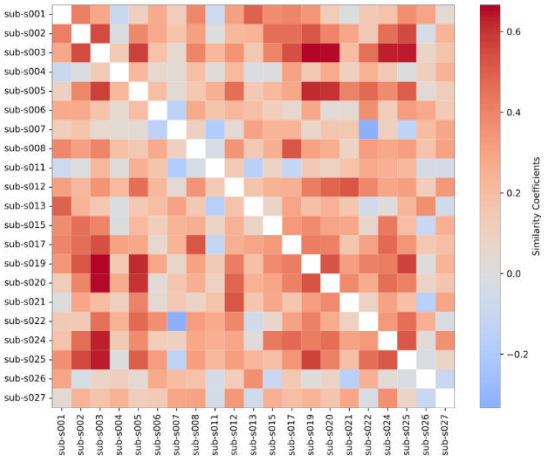
Spearman's rank (rho) Similarity Coefficients for the Regions with most Between-Subject Variance

a) Per Subject Mean Similarity Coefficient



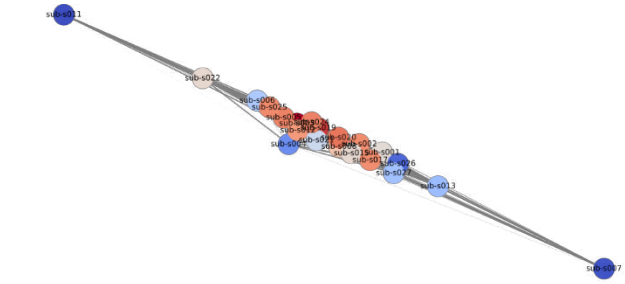
Mean Spearman's rank (rho) similarity coefficient for each subject over all pairwise comparisons including confidence intervalls (95%). Mean similarity was rho = 0.23 (SD=0.09), range=0.30. Smallest similarity showed subject sub-s011 with rho = 0.068, highest subject sub-s019 with rho = 0.349.

b) Subject x Subject Similarity Matrix



The matrix shows the Spearman Similarity Coeficients of the pairwise comparisons between subjects. Darker red fields indicate a higher similarity, while lighter fields to blue present a lower similarity. The highest similarity was observed between subject sub-s003 and sub-s019 with rho = 0.666, the lowest similarity showed the comparison between subject sub-s007 and subject sub-s022 with rho = -0.333.

c) Network Representation of the Similarity



In this network the length and thickness of the connections between two subjects represent their similarity value, thus, thicker and shorter lines indicate higher similarity beetween two subjects, while thiner and longer lines illustate lower similarity.

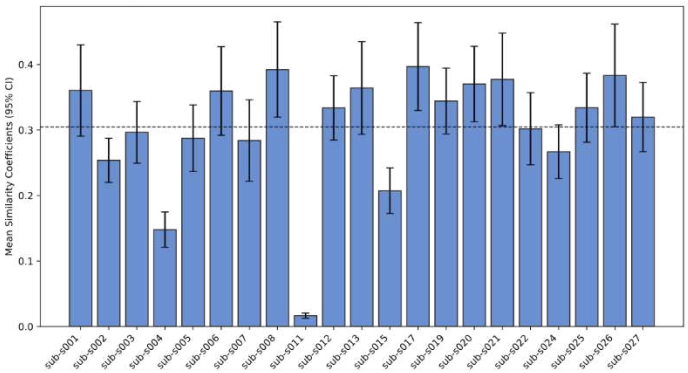
Across all pairwise comparisons, the mean Jaccard coefficient (J) was J = 0.31 (SD = 0.09), with a range of 0.38. Subject-specific mean pairwise similarity was lowest for subject sub-s011 (J = 0.017, SD = 0.01), followed by sub-s004 (J = 0.148, SD = 0.06), and s015 (J = 0.207, SD = 0.08). The highest mean pairwise similarity was observed for sub-sub-s017 (J = 0.397, SD = 0.14). Compare Fig. 6.

We again checked for a possible correlation between noise parameters and similarity coefficients and could not identify one.

Fig. 6

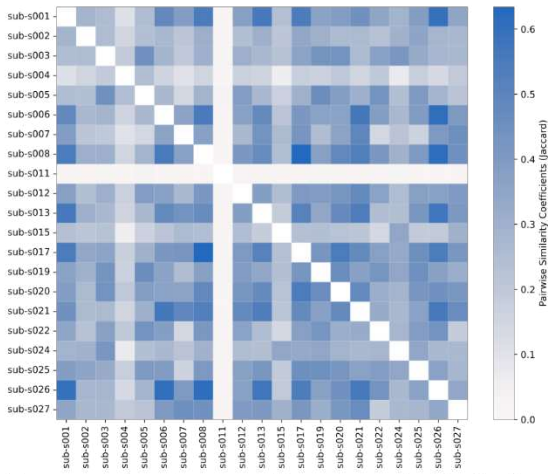
Jaccard Similarity Coefficients for the Regions with the most Between-Subject Variance

a) Per Subject Mean Similarity Coefficient



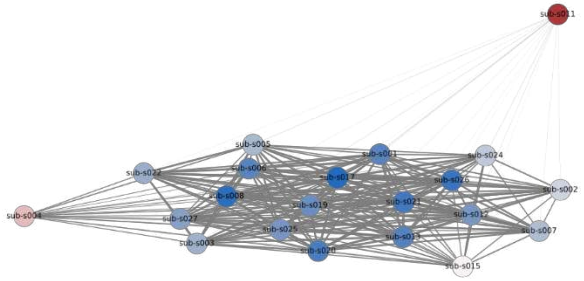
Mean Jaccard similarity coefficient for each subject over all pairwise comparisons including confidence intervalls (95%). Mean similarity was J = 0.31 (SD=0.09), range=0.38. Smallest similarity showed subject sub-s011 with J = 0.017, highest subject sub-s017 with J = 0.397.

b) Subject x Subject Similarity Matrix



The matrix shows the Jaccard Similarity Coeficients of the pairwise comparisons between subjects. Darker fields indicate a higher similarity, while lighter field present a lower similarity. The highest similarity was observed between subject sub-s008 and sub-s017 with J = 0.634, the lowest similarity showed the comparison between subject sub-s004 and sub-s011 with J = 0.017.

c) Network Representation of the Similarity Coefficients



In this network the length and thickness of the connections between two subjects represent their similarity value, thus, thicker and shorter lines indicate higher similarity beetween two subjects, while thiner and longer lines illustate lower similarity.

3.3 Similarity Coefficients and Participant Characteristics

Across the three word-discrimination tasks, participants correctly identified target stimuli in 89.2% of trials (SD = 8.86%), compared with 95.3% (SD = 6.76%) in the false-font control condition. Mean reaction time was 0.758 s (SD = 0.088 s) for word discrimination and 0.553 s (SD = 0.073 s) for the control condition. Performance was significantly higher in the control condition (t = −5.1, p < .001, mean difference = −6.04%, d = −1.11), and responses were significantly faster (t = 22.4, p < .001, mean difference = 0.204 s, d = 4.88). Task performance, either in response accuracy or speed, did not correlate with any similarity measure.

In the SLRT-2, participants read on average 120.4 words (SD = 18.63), of which 98.0% (SD = 1.36) were read correctly, and 76.2 pseudowords (SD = 20.97), with 95.8% (SD = 3.07)

correct. In the SLS, participants read an average of 53.29 sentences (SD = 11.31), with 97.4% (SD = 6.61) correct semantic judgements. Mean scores on the four WAIS-IV subtests were 21.6 (SD = 2.58) for Matrix Reasoning, 35.1 (SD = 4.92) for Digit Span, 47.3 (SD = 5.39) for Vocabulary, and 87.0 (SD = 15.10) for Coding. No significant correlation between these measurements and the similarity coefficients could be identified on the whole brain level. However, the Jaccard coefficient for the regions included in the most between-subject variance mask correlated negatively with the number of sentences processed in the SLS (Pearson's r = -0.60, p=.004). Additionally, we checked for a possible correlation between the similarity coefficients and age or educational level of the subjects and could not identify one.

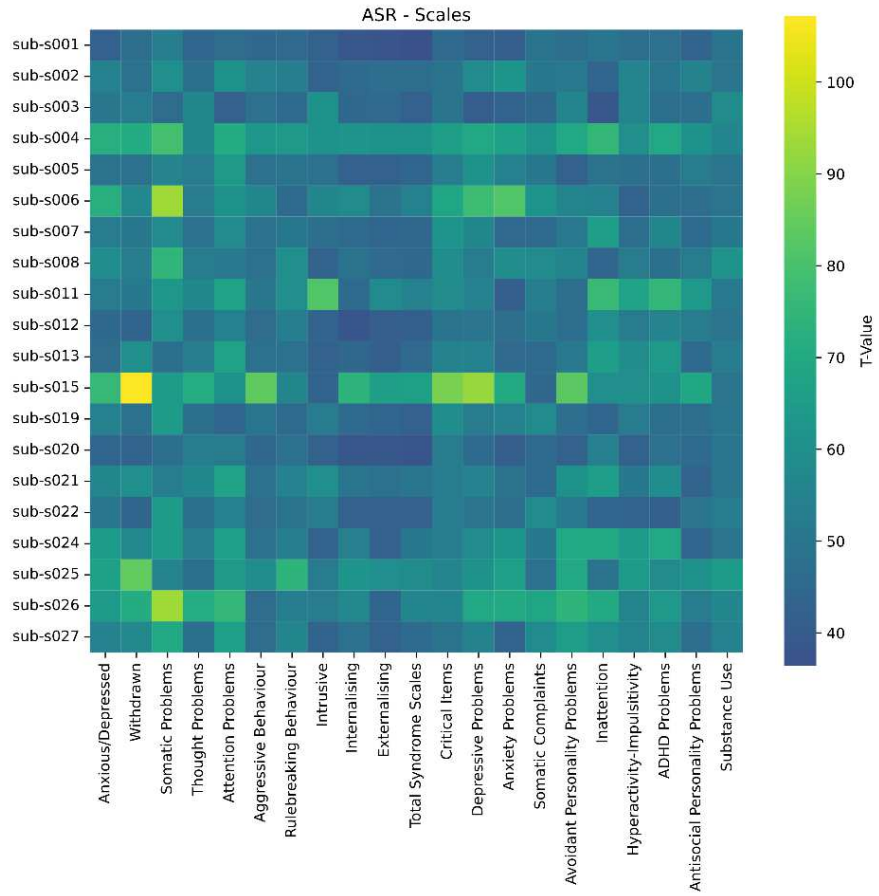
We assessed the subjects' mental health using the Adult Self-Report (ASR) (Achenbach and Rescorla 2003). Most had T-scores within the normal range. At group level, only the Somatic Problems scale had an increased mean score (mean T = 63.32, SD = 13.51). High individual scores (T > 80) were observed for sub-s006 and sub-s026 on the Somatic Problems scale (both T = 93.42), sub-s011 on the Intrusive scale (T = 81.69), and sub-s015 on the Withdrawn (T = 107.18) and Aggressive Behaviour (T = 84.10) scales. Participants sub-s004, sub-s006, sub-s015, and sub-s026 had elevated scores (T > 60) across multiple scales (see Fig. 7 for details). The concrete scores of each subject can be found in Table A2 and A3 of the Appendix.

We further examined whether psychopathological scores were associated with inter-subject similarity by correlating the ASR scales with both similarity measures. The Jaccard coefficients were negatively associated with several attention-related scales: the Hyperactivity–Impulsivity scale (whole brain: r = −0.59, p = .006; most between-subject variance regions: r = −0.56, p = .010) and the ADHD Problems scale (whole brain: r = −0.59, p = .006; most between-subject variance regions: r = −0.58, p = .008). There was also a significant correlation between the ADHD Problems scale and Spearman's rho (most between-subject variance regions: r = −0.56, p = .10). Similarly, the Attention Problems syndrome scale (r = −0.62, p = .004) and the Inattention scale (most between-subject variance regions: r = −0.73, p < .001) were significantly correlated with Spearman's rho. Another group of scales showing significant correlations with the Jaccard index were Externalising (whole brain: r = −0.57, p = .009; most between-subject variance regions: r = −0.62, p = .004), Antisocial Personality Problems scale (whole brain: r = −0.66, p = .002; most between-subject variance regions: r = −0.66, p = .006) and Aggressive Behaviour (whole brain: r = −0.57, p = .009). Additionally, Spearman's rho correlated negatively with the Mean Substance Use (whole brain: r = 0.59, p = .006) and the Jaccard index with the Intrusive scale (most between-subject variance regions: r = 0.60, p = .005). Higher scores

on all these ASR scales were associated with lower similarity of activation patterns between participants.

Fig. 7

Distribution of Adult Self-Report (ASR) T-score



Heatmap of individual participants' ASR T-scores across the syndrome and DSM-oriented scales as well as the mean substance use. Each row represents one participant and each column one ASR scale. Colours represent T-scores, ranging from dark blue (lower values) to yellow (higher values). Scores of T > 60 represent clinically noticeable elevations.

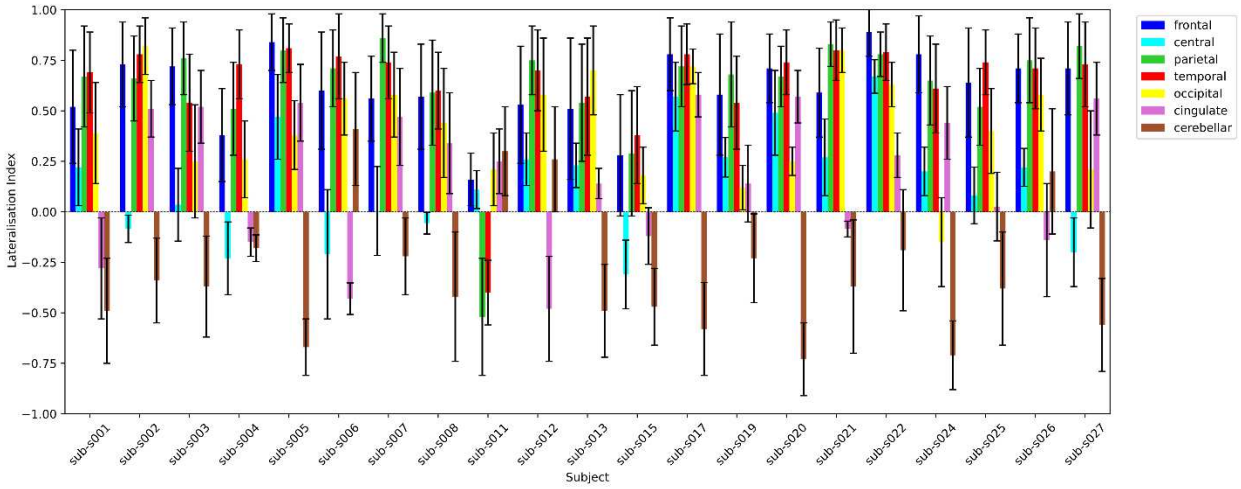
3.4 Lateralisation Index

We further calculated the Lateralisation Index (LI) for the cortex and found a left lateralisation in most cortices, except for the cerebellum. One subject (sub-s011) showed clear right lateralisation in the parietal and temporal lobe, and another (sub-s024) in the occipital cortex (see Fig. 8). There was no significant difference in lateralisation between the sexes, and no correlation between task performance and LI. The Jaccard coefficient correlated with lateralisation of activity in the parietal (Pearson's r = 0.62, p = .002) and temporal lobe (Pearson's r = 0.58, p = .006). We repeated this process for regions with the

most between-subject variance, finding a correlation with lateralisation in the frontal (Pearson's r = 0.59, p = .005), the parietal (Pearson's r = 0.76, p < .001) and temporal cortex (Pearson's r = 0.71, p < .001).

Fig. 8

Lateralisation indices across participants and cortices



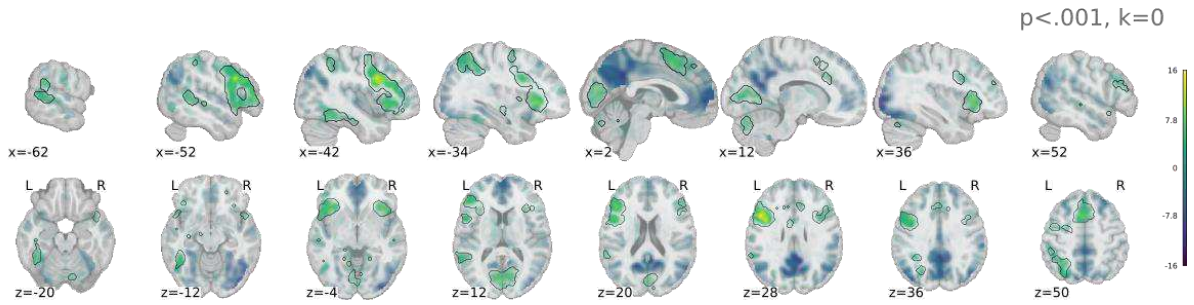
Lateralisation indices (LI) for each participant are shown for the frontal, central, parietal, temporal, occipital, and cingulate cortices, as well as the cerebellum. Positive LI values indicate left-lateralised activation, whereas negative values indicate right-lateralised activation. Error bars represent the 95% confidence interval of the LI.

3.5 Group Level Analysis

Group-level analysis revealed bilateral activity in the IFG, frontal operculum, calcarine cortex, SMG, anterior insula, lingual gyrus, cuneus, and left lateralised activity in the precentral gyrus, MFG, STG, SMG, SPL, ITL, MFG, fusiform gyrus, AnG, and SFG, and right lateralised activity in the cerebellum for visual word processing (see Fig. 9).

Fig. 9

Group level activation for the contrast all decision tasks vs. control task (false font), significant activation (p<.001) is encircled with a black line, no cluster extent threshold was applied.

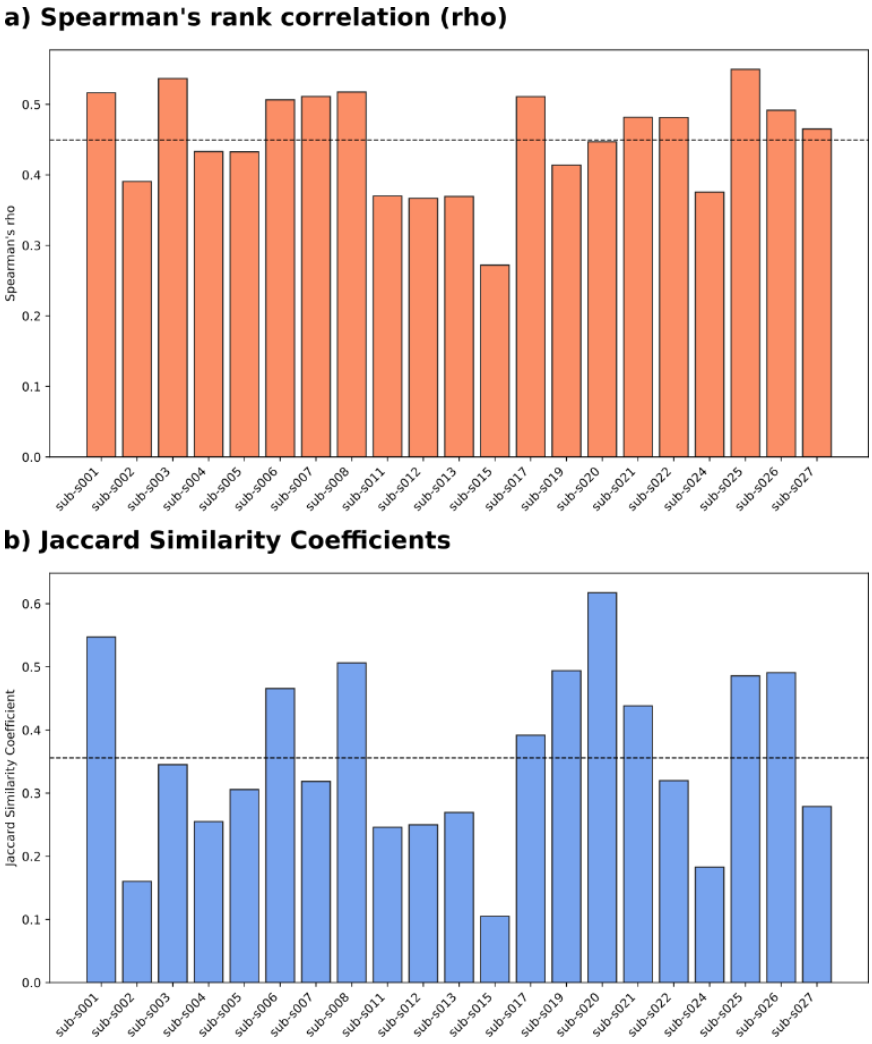


We investigated how closely each participant's activation pattern resembled the group-level activation pattern. We calculated the similarity between each participant's activation map and the group activation map using Spearman's rho and the Jaccard coefficient. Across participants, mean rho was 0.45 (SD = 0.07). Subjects with below-average similarity were sub-s015 (rho = 0.27), followed by sub-s011, sub-s012, sub-s013, and sub-s024 (each rho = 0.37). Highest similarity with the group-level map showed sub-s025 (rho = 0.55), followed by sub-s003 (rho = 0.54).

The mean Jaccard coefficient was 0.36 (SD = 0.14). Remarkably low Jaccard coefficients showed subject sub-s015 (J = 0.11), sub-s002 (J = 0.16), and sub-s024 (J = 0.18). Highest was sub-s020 (J = 0.62), followed by sub-s001 (J = 0.55) and sub-s008 (J = 0.51) (see Fig. 10).

Fig. 10

Similarity between individual- and group-level activation maps



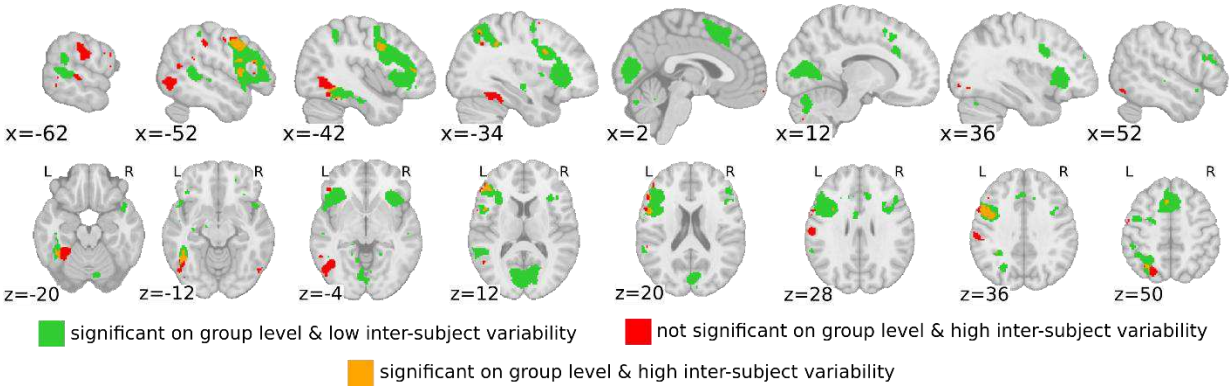
a) Similarity quantified by Spearman's rho, reflecting the similarity of the relative activation pattern across voxels. b) Similarity quantified by the Jaccard coefficient, reflecting the spatial overlap of significant voxels. Bars represent the similarity coefficient for each participant, and dashed horizontal lines indicate the corresponding group mean (Spearman's rho = 0.45; Jaccard coefficient = 0.36).

We compared the regions we classified as most between-subject variance regions with the group activation map, identifying at least a partial overlap in several regions, including the precentral gyrus, IFG pars triangularis and opercularis, ITG, IPL, SPL, fusiform gyrus, MFG and AnG. Most clusters identified within the mask were rather small (<100voxel), except for the precentral gyrus (cluster size 272; AAL atlas). The mask also included areas not classified as active in the group analysis, which include parts of the left fusiform gyrus, left ITG, MTG and STG, left postcentral gyrus, left SMG, left SPL, bilateral iOT, left precentral gyrus, left mOT, and left IFG pars triangularis and opercularis. Note that in the fusiform

gyrus, the left iOT, the postcentral gyrus and MTG, the cluster size exceeded 100 voxels. Also compare Fig. 11.

Fig. 11

Overlay of group level activation map (p <. 001) and mask of most between-subject variance (ICC > 0.6 and top 5% of between-subject variance).



4. Discussion

The study investigated variability in neural activity during written word processing. The similarity between the individuals' neural activation patterns was assessed and we identified regions with most variance in activity between subjects and possible relations to subjects' characteristics. The final stage of the analysis entailed the examination of group-level activation maps in relation to between-subject variability.

4.1 Between-Subject Similarity

We identified low to moderate similarity between the activation maps of the individual subjects. Spearman's rho averaged at 0.26, and the thresholded maps achieved only 16% voxel overlap. However, the voxel overlap index depends on the threshold used; in our case, the threshold was strict ($p < .001$). The low to moderate overall similarity in activation during word processing indicates substantial differences in functional topography between individuals. The next question to address is the location of these discrepancies.

4.2 Regions with most Between-Subject Variance

The regions showing the greatest between-subject variance substantially overlap with the known language network, including the IFG pars triangularis and opercularis, the precentral gyrus, the STG, the MFG, the SMA, the MTG, the vOT, the AnG, and the cerebellum. However, they also encompass neighbouring regions such as the postcentral gyrus, the SPL, the mOT, the iOT, the plenum temporale, and the ITG.

The variability among individuals within these regions may be a contributing factor to the ongoing debate surrounding the precise function of these regions. For example, there is inconclusive data regarding a posterior-to-anterior functional gradient within the IFG, with the pars opercularis associated with phonological and articulatory processing, and the pars triangularis and pars orbitalis support semantic retrieval and lexical selection (Glezer et al. 2016; Yuan et al. 2023; Pattamadilok et al. 2017; Turker and Hartwigsen 2021; Turker et al. 2023; Hodgson et al. 2021; Yu et al. 2018; Cone et al. 2008; Hartwigsen et al. 2010; Goucha and Friederici 2015). Moreover, parts of the IFG could belong to the domain-general, multiple-demand network that is activated during cognitively demanding tasks (Braga et al. 2020; Hodgson et al. 2021). Similarly, the AnG is mostly linked to semantic processing, while some researchers have associated the AnG with phonological processing (Hodgson et al. 2021; Weber et al. 2020; Turker et al. 2023; Ravenschlag et al. 2024; Glezer et al. 2016; Martin et al. 2015; Yu et al. 2018) and others have not identified a clear distinction between the two processes (Turker et al. 2023). The network affiliation of the AnG is also in question: more recent evidence suggests that it is rather part of the default mode network (Turker et al. 2023; Braga et al. 2020; Hodgson et al. 2021).

The high between-subject variance we observed therefore suggest that the distinct functional assignment of these regions and their subregions may vary considerably from one individual to another. This would grant those regions a more flexible functional role in the overall functional topography of the brain.

We assessed similarity between subjects specifically within the regions showing the greatest interindividual variance. While the similarity was comparable to the whole-brain level, both similarity measures exhibited greater range among individuals within these regions (rho 0.16 vs. 0.30; Jaccard 0.11 vs. 0.38). This heterogeneity was particularly pronounced for the voxel overlap ranging from ~2% to ~40%. However, the substantially smaller number of voxels included in the ROI analysis may have contributed to the wider range of similarity estimates. Nevertheless, the overall pattern indicated that, in these regions, a small number of subjects exhibited remarkably different activation patterns. While our results suggest a few extreme outliers, the sample size is insufficient to determine whether these represent distinct subgroups of individuals.

4.3 Between-Subject Variance and Subject Characteristics

Surprisingly, we found no significant correlation between task performance and neural similarity during word processing. Participants consistently performed the task well, potentially due to the low task demands. Therefore, the absence of an association in our study does not negate the possibility of a relationship between variability in neural activity and task performance. Indeed, neural similarity was associated with performance on an

independent reading test in areas displaying the greatest variability in neural activity across subjects. Higher reading ability was linked with lower neural similarity in these areas. Further clarification of this relationship requires tasks with greater cognitive demands and more thorough reading ability assessments.

Beyond reading ability, we also examined how individual differences in psychological traits are reflected in the similarity of participants' neural activity. Those with higher levels of attention problems (Hyperactivity/impulsivity, ADHD-related problems and inattention) and antisocial traits (externalising problems, antisocial personality, and aggressive behaviour) exhibited lower neural similarity. Importantly, these associations were observed in a non-clinical sample, indicating that variation in psychopathological traits is reflected in individual differences in brain function even in the absence of a clinical diagnosis. While this study only explorative described potential relations, future studies using precision fMRI in combination with dimensional psychopathological assessments, could significantly advance our understanding of brain–behaviour relations.

4.4 Lateralisation and Between-Subject Variance

Alterations in the language networks lateralisation is a known variation between individuals (Andrulyte et al. 2026; Seghier and Price 2018). In our study two subjects (sub-s011 and sub-s024) exhibited right-lateralised activation. The correlation between the Lateralization Index of the parietal and temporal lobe with the Jaccard index hints that individual differences in the spatial distribution of activity are at least partially due to lateralization differences.

Notably, sub-s024 exhibited right lateralisation only in the occipital cortex. Therefore, lateralisation within the language network may follow a modular principle, whereby components of the network can vary independently. This variation is important for interpreting activation patterns at the group level. Group-level averaging can underestimate the prevalence and magnitude of activation when the lateralisation of the response to a stimulus varies between individuals. This might be relevant for the language network especially since a weaker homologous right lateralised part has been proposed.

4.5 Individual Activation Patterns and Group Level Analysis

Our study also aimed to evaluate how well group-level activation maps represent individual participants' neural activation patterns. We observed a moderate similarity between participants' activation patterns and the group-level activation pattern (rho = 0.45). Voxel-wise overlap was also moderate at 36%. However, each participant's map contributes to the group-level map, meaning the measures are not independent. The

moderate correspondence suggests that group-level activation maps may not fully represent true underlying activation patterns.
We therefore examined which regions may be insufficiently represented by the group-level analysis. Most of the regions showing the greatest between-subject variance overlapped (parts of the left-lateral precentral gyrus, the IFG pars triangularis and opercularis, the ITG, the IPL, the SPL, the fusiform gyrus, the MFG, and the AnG) or were adjacent (parts of the left fusiform gyrus, the ITG, the MTG, the STG, the pre- and postcentral gyrus, the SMG, the SPL, the iOT, the mOT, and the IFG pars triangularis and opercularis) to the regions identified within the group analysis. This shows how important it is to remember what a group-level result represents: an active region resembles an average after all participants have been aggregated. However, this does not mean that every subject exhibited this pattern. While a group-level map reveals the network's common spatial framework, individual-level analyses depict how activation varies within that framework.
Discrepancies between group-level and individual activation maps do not mean that group-level analyses are inadequate, but rather that they provide a different perspective on neural activation.
Therefore, rather than suggesting entirely distinct patterns of neural activity across individuals, our findings are more consistent with the idea that there are individual differences in the precise spatial distribution and extent of activation within a broadly shared language network. The current model of the language network may provide a valid approximation of the neural organisation across people but does not fully capture activation at the individual level. However, a broad characterisation of the language network may suffice for questions concerning its general organisation, but greater precision on the individual level may be necessary when investigating more specific research questions. This could include the relationship between neuropsychological traits and neural activity, or the development of personalised treatments.

5. Conclusion

Overall, our findings demonstrate a common language network across individuals, alongside substantial interindividual variability in the functional organisation in parts of this network between individuals. This variability also encompasses differences in hemispheric lateralisation and is associated with reading performance and psychopathological traits. Importantly, group-level activation patterns resembled the individual level patterns only moderately, not capturing such variations. Therefore, incorporating individual-level functional organisation alongside conventional group-level analyses will provide a more precise characterisation of the language network and its relationship to behaviour in the future.

Data and Code Availability

The ANC language study dataset is available through the Austrian NeuroCloud (https://anc.plus.ac.at/) at: *https://doi.org/10.60817/39tp-6031*. The ANC is a research data repository designed for FAIR and trustworthy data management in neuroscience. The dataset contains MRI images from which facial features could be reconstructed. In compliance with the GDPR, data that may carry personal information cannot be made publicly available. Access to this dataset is restricted but may be granted for research and educational purposes upon request. For details, please refer to the ANC.

The experimental code, stimuli and MRIQC results are available at osf: *10.17605/OSF.IO/W7BFA*.

References

Achenbach TM, Rescorla LA (2003) Manual for the ASEBA Adult Forms & Profiles. Burlington. VT: University of Vermont, Research Center for Children, Youth, & Families,

Andrulyte I, Zago L, Jobard G, Lemaitre H, Taylor PN, Rheault F, Joliot M, Petit L, Keller SS (2026) Brain structure—function coupling — relationship with language lateralisation. Cortex 204:115—132. doi:10.1016/j.cortex.2026.08.001

Billingsley RL, McAndrews MP, Crawley AP, Mikulis DJ (2001) Functional MRI of phonological and semantic processing in temporal lobe epilepsy. Brain 124. doi:doi.org/10.1093/brain/124.6.1218

Braga RM, DiNicola LM, Becker HC, Buckner RL (2020) Situating the left-lateralized language network in the broader organization of multiple specialized large-scale distributed networks. J Neurophysiol 124. doi:10.1152/jn.00753.2019.

Caballero-Gaudes C, Moia S, Panwar P, Bandettini PA, Gonzalez-Castillo J (2019) A deconvolution algorithm for multi-echo functional MRI: Multi-echo Sparse Paradigm Free Mapping. NeuroImage 202. doi:10.1016/j.neuroimage.2019.116081

Casto C, Poliak M, Tuckute G, Small H, Sherlock P, Wolna A, Lipkin B, D'Mello AM, Fedorenko E (2026) The cerebellar components of the human language network. Neuron 114:1504–1523. doi:10.1016/j.neuron.2025.12.030

Cone NE, Burman DD, Bitan T, Bolger DJ, Booth JR (2008) Developmental changes in brain regions involved in phonological and orthographic processing during spoken language processing. NeuroImage 41. doi:10.1016/j.neuroimage.2008.02.055

Cui Z, Su M, Shu LL, Gong G (2018) Individualized Prediction of Reading Comprehension Ability Using Gray Matter Volume. Cerebral Cortex 28:1656–1672. doi:10.1093/cercor/bhx061

DuPre E, Salo T, Ahmed Z, Bandettini PA, Bottenhorn KL, Caballero-Gaudes C, Dowdle LT, Gonzalez-Castillo J, Heunis S, Kundu P, Laird AR, Markello R, Markiewicz CJ, Moia S, Staden I, Teves JB, Uruñuela E, Vaziri-Pashkam M, Whitaker K, Handwerker DA (2021) TE-dependent analysis of multi-echo fMRI with tedana. Journal of Open Source Software 6. doi:10.21105/joss.03669

Elliott ML, Knodt AR, Hariri AR (2021) Striving toward translation: strategies for reliable fMRI measurement. Trends in Cognitive Science 25 (9). doi:10.1016/j.tics.2021.05.008

Esteban O, Birman D, Schaer M, Koyejo OO, Poldrack RA, Gorgolewski KJ (2017) MRIQC: Advancing the Automatic Prediction of Image Quality in MRI from Unseen Sites. PLOS ONE 12 (9). doi:10.1371/journal.pone.0184661

Esteban O, Markiewicz CJ, Blair RW, Moodie CA, Isik AI, Erramuzpe A, Kent JD, Goncalves M, DuPre E, Snyder M, Oya H, Ghosh SS, Wright J, Durnez J, Poldrack RA, Gorgolewski KJ (2019) fMRIPrep: a robust preprocessing pipeline for functional MRI. Nature Methodes 11:111-116. doi:10.1038/s41592-018-0235-4

Fedorenko E (2021) The early origins and the growing popularity of the individual-subject analytic approach in human neuroscience. Current Opinion in Behavioral Sciences 40:105-112. doi:10.1016/j.cobeha.2021.02.023

Fedorenko E, Ivanova AA, Regev TI (2024) The language network as a natural kind within the broader landscape of the human brain. Nature Reviews Neuroscience 25. doi:10.1038/s41583-024-00802-4

Glezer LS, Eden G, Jiang X, Luetje M, Napoliello E, Kim J, Riesenhuber M (2016) Uncovering phonological and orthographic selectivity across the reading network using fMRI-RA. NeuroImage 138. doi:10.1016/j.neuroimage.2016.05.072

Goucha T, Friederici AD (2015) The language skeleton after dissecting meaning: A functional segregation within Broca's Area. Neuroimage 114:294-302. doi:10.1016/j.neuroimage.2015.04.011

Granocchio E, De Salvatore M, Bonanomi E, Sarti D (2021) Sex- related differences in reading achievement. Journal of Neuroscience Research 101. doi:10.1002/jnr.24913

Gratton C, Kraus BT, Greene DJ, Gordon EM, Laumann TO, Nelson SM, Dosenbach NUF, Petersen SE (2020) Defining Individual-Specific Functional Neuroanatomy for Precision Psychiatry. Biological Psychiatry 88. doi:10.1016/j.biopsych.2019.10.026

Hartwigsen G, Price CJ, Baumgaertner A, Geiss G, Koehnke M, Ulmer S, Siebner HR (2010) The right posterior inferior frontal gyrus contributes to phonological word decisions in the healthy brain: Evidence from dual-site TMS. Neuropsychologia 48. doi:10.1016/j.neuropsychologia.2010.06.032

Hawelka S, Wimmer H (2008) Visual target detection is not impaired in dyslexic readers. Vision Research 48:850–852. doi:10.1016/j.visres.2007.11.003

Hodgson VJ, Lambon Ralph MA, Jackson RL (2021) Multiple dimensions underlying the functional organization of the language network. NeuroImage 241. doi:doi.org/10.1016/j.neuroimage.2021.118444

Jung M, Mody M, Fujioka T, Kimura Y, Okazawa H, Kosaka H (2019) Sex Differences in White Matter Pathways Related to Language Ability. frontiers in neuroscience 13. doi:10.3389/fnins.2019.00898

Kirilina E, Lutti A, Poser BA, Blankenburg F, Weiskopf N (2016) The quest for the best: The impact of different EPI sequences on the sensitivity of random effect fMRI group analyses. NeuroImage 126. doi:10.1016/j.neuroimage.2015.10.071

Korucuoglu O, Harms MP, Astafiev SV, Kennedy JT, Golosheykin S, Barch DM, Anokhin AP (2020) Test-retest reliability of fMRI-measured brain activity during decision making under risk. NeuroImage 214. doi:10.1016/j.neuroimage.2020.116759

Kronbichler M, Bergmann J, Hutzler F, Staffen W, Mair A, Ladurner G, Wimmer H (2007) Taxi vs. Taksi: On orthographic word recognition in the left ventral occipitotemporal cortex. Journal of Cognitive Neuroscience 19 (10)

Kundu P, Voon V, Balchandani P, Lombardo MV, Poser BA, Bandettini PA (2017) Multi-echo fMRI: A review of applications in fMRI denoising and analysis of BOLD signals. NeuroImage 154. doi:10.1016/j.neuroimage.2017.03.033

Laumann TO, Gordon EM, Adeyemo B, Snyder AZ, Joo SJ, Chen M-Y, Gilmore AW, McDermott KB, Nelson SM, Dosenbach NUF, Schlaggar BL, Mumford JA, Poldrack RA, Petersen SE (2015) Functional System and Areal Organization of a Highly Sampled Individual Human Brain. Neuron 87. doi:10.1016/j.neuron.2015.06.037

Liu X, Hu Y, Hao Y, Yang L (2024) Individual differences in the neural architecture in semantic processing. scientific reports 14. doi:10.1038/s41598-023-49538-8

Liuzzi AG, Bruffaerts R, Vandenberghe R (2019) The medial temporal written word processing system. Cortex 119:287-300. doi:10.1016/j.cortex.2019.05.002

Ludersdorfer P, Wimmer H, Richlan F, Schurz M, Hutzler F, Kronbichler M (2016) Left ventral occipitotemporal activation during orthographic and semantic processing of auditory words. NeuroImage 124. doi:10.1016/j.neuroimage.2015.09.039

Lüdtke J, Froehlich E, Jacobs AM, Hutzler F (2019) The SLS-Berlin: Validation of a German Computer-Based Screening Test to Measure Reading Proficiency in Early and Late Adulthood. Frontiers in Psychology 10. doi:10.3389/fpsyg.2019.01682

Lynch CJ, Elbau I, Liston C (2021) Improving precision functional mapping routines with multi-echo fMRI. Current Opinion in Behavioral Sciences 40. doi:10.1016/j.cobeha.2021.03.017

Lynch CJ, Power JD, Scult MA, Dubin M, Gunning FM, Liston C (2020) Rapid Precision Functional Mapping of Individuals Using Multi-Echo fMRI. Cell Reports 33. doi:10.1016/j.celrep.2020.108540

Martin A, Schurz M, Kronbichler M, Richlan F (2015) Reading in the Brain of Children and Adults: A Meta-Analysis of 40 Functional Magnetic Resonance Imaging Studies. Human Brain Mapping 36. doi:10.1002/hbm.22749

Michon KJ, Khammash D, Simmonite M, Hamlin AM, Polk TA (2022) Person-specific and precision neuroimaging: Current methods and future directions. NeuroImage 263. doi:10.1016/j.neuroimage.2022.119589

Moia S, Termenon M, Uruñuela E, Chen G, Stickland RC, Bright MG, Caballero-Gaudes C (2021) ICA-based denoising strategies in breath-hold induced cerebrovascular reactivity mapping with multi echo BOLD fMRI. NeuroImage 233. doi:10.1016/j.neuroimage.2021.117914

Moliadze V, Stenner T, Matern S, Siniatchkin M, Nees F, Hartwigsen G (2021) Online Effects of Beta-tACS Over the Left Prefrontal Cortex on Phonological Decisions. Neuroscience 463. doi:10.1016/j.neuroscience.2021.03.002
Moll K, Landerl K (2014) SLRT-II: Lese- und Rechtschreibtest; Weiterentwicklung des Salzburger Lese- und Rechtschreibtests (SLRT). 2 edn. Huber, Hogrefe., Bern, Germany
Pattamadilok C, Chanoine V, Pallier C, Anton J-L, Nazarian B, Belin P, Ziegler JC (2017) Automaticity of phonological and semantic processing during visual word recognition. NeuroImage 149:244–255. doi:10.1016/j.neuroimage.2017.02.003
Petermann F (ed) (2018) Wechsler adult intelligence scale - fourth edition : WAIS-IV. deutschsprachige Adaption nach David Wechsler (3rd ed.). Pearson,
Planton S, Chanoine V, Sein J, Anton J-L, Nazarian B, Pallier C, Pattamadilok C (2019) Top-down activation of the visuo-orthographic system during spoken sentence processing. NeuroImage 202. doi:10.1016/j.neuroimage.2019.116135
Poldrack RA (2017) Precision Neuroscience: Dense Sampling of Individual Brains. Neuron 95. doi:10.1016/j.neuron.2017.08.002
Prat CS, Gallée J, Yamasaki BL (2023) Getting language right: Relating individual differences in right hemisphere contributions to language learning and relearning. Brain & Language 239. doi:10.1016/j.bandl.2023.105242
Ravenschlag A, Denissen M, Kronbichler L, Kronbichler M (2024) Orthographic processing. Neuroscience and Biobehavioral Psychology. doi:10.1016/B978-0-12-820480-1.00139-X
Seghier ML, Lazeyras F, Pegna AJ, Annoni J-M, Zimine I, Mayer E, Michel CM, Khateb A (2004) Variability of fMRI Activation During a Phonological and Semantic Language Task in Healthy Subjects. Human Brain Mapping 23. doi:10.1002/hbm.20053
Seghier ML, Price CJ (2018) Interpreting and Utilising Intersubject Variability in Brain Function. Trends in Cognitive Science 22 (6). doi:10.1016/j.tics.2018.03.003
Smith DM, Perez DC, Porter A, Dworetsky A, Gratton C (2021) Light through the fog: using precision fMRI data to disentangle the neural substrates of cognitive control. Current Opinion in Behavioral Sciences 40. doi:10.1016/j.cobeha.2020.12.004
Spencer M, Cutting LE (2021) Relations among Executive Function, Decoding, and Reading Comprehension: An Investigation of Sex Differences. Discourse Processes 58 (1). doi:10.1080/0163853X.2020.1734416
Steckermeier E, Kronbichler M, Hutzler F, Braun M (2025a) ANC language study [Data set] (Commit: b735fedb). Austrian NeuroCloud. doi:10.60817/39tp-6031)
Steckermeier E, Kronbichler M, Hutzler F, Braun M (2025b) Austrian NeuroCloud language study [Supplementary material]. Open Science Framework. https://doi.org/10.60817/39tp-6031.
Steckermeier EP, Kronbichler M, Hutzler F, Braun M (2026) ANC language study: A multi-session, multi-echo fMRI dataset for individual level language research. ApertureNeuro 6 (SI 1). doi:10.52294/001c.155650
Steel A, Garcia BD, Silson EH, Robertson CE (2022) Evaluating the efficacy of multi-echo ICA denoising on model-based fMRI. NeuroImage 264. doi:10.1016/j.neuroimage.2022.119723

Turker S, Hartwigsen G (2021) Exploring the neurobiology of reading through non-invasive brain stimulation: A review. Cortex 141. doi:10.1016/j.cortex.2021.05.001
Turker S, Kuhnke P, Eickhoff SB, Caspers S, Hartwigsen G (2023) Cortical, Subcortical, and Cerebellar Contributions to Language Processing: A Meta-Analytic Review of 403 Neuroimaging Experiments. Psychological Bulletin 149:699–723. doi:10.1037/bul0000403
Vanova M, Aldridge-Waddon L, Jennings B, Puzzo I, Kumari V (2020) Reading skills deficits in people with mental illness: A systematic review and meta-analysis. European Psychiatry 64 (1):1–28. doi:10.1192/j.eurpsy.2020.98
Wagley N, Booth JR (2022) Neural pathways of phonological and semantic processing and its relations to children's reading skills. Frontiers in Neuroscience. doi:10.3389/fnins.2022.984328
Weber S, Hausmann M, Kane P, Weis S (2020) The relationship between language ability and brain activity across language processes and modalities. Neuropsychologia 146. doi:10.1016/j.neuropsychologia.2020.107536
Wilke M, Lidzba K (2007) LI-tool: A new toolbox to assess lateralization in functional MR-data. Journal of Neuroscience Methods 163:128–136. doi:10.1016/j.jneumeth.2007.01.026
Xu M, Liang X, Ou J, Li H, Luo Y-j, Tan LH (2020) Sex Differences in Functional Brain Networks for Language. Cerebral Cortex 30. doi:10.1093/cercor/bhz184
Yamasaki BL, Prat CS (2023) Individual Differences in Inhibitory Control Relate to Neural Efficiency During Reading. Mind, Brain, and Education 17 (4). doi:10.1111/mbe.12382
Yu M, Wu Z, Luan M, Wang X, Song Y, Liu J (2018) Neural correlates of semantic and phonological processing revealed by functional connectivity patterns in the language network. Neuropsychologia 121. doi:10.1016/j.neuropsychologia.2018.10.027
Yuan B, Xie H, Wang Z, Xu Y, Zhang H, Liu J, Chen L, Li C, Tan S, Lin Z, Hu X, Gu T, Lu J, Liu D, Wu J (2023) The domain-separation language network dynamics in resting state support its flexible functional segregation and integration during language and speech processing. NeuroImage 274. doi:10.1016/j.neuroimage.2023.120132
Zhang X, Liang M, Qin W, Wan B, Yu C, Ming D (2020) Gender Differences Are Encoded Differently in the Structure and Function of the Human Brain Revealed by Multimodal MRI. Frontiers in Human Neuroscience 14. doi:10.3389/fnhum.2020.00244

Statements and Declarations

Funding

This work was supported by the Austrian NeuroCloud (ANC) under grant number 2920, funded by the Federal Ministry of Education, Science and Research (BMBWF).

Competing Interests

The authors have no competing interests to declare.

Authors Contributions

The conceptualisation and methodology of the study were contributed to by Eva P. Steckermeier, Mario Braun and Martin Kronbichler. The formal analysis and curation of the data was conducted by Eva P. Steckermeier, who was also responsible for the original draft and the creation of all visualisations. The supervision, project administration, and the reviewing and editing of the writing was carried out by Martin Kronbichler. The responsibility for the acquisition of resources and funding lay with Florian Hutzler and Martin Kronbichler.

Supplementary Files

This is a list of supplementary files associated with this preprint. Click to download.

- APPENDIX.docx